Proceedings of the 2003 IEEE/RSJ
Intl. Conference on Intelligent Robots and Systems
Las Vegas, Nevada · October 2003

A Wire-Driven Miniature Five Fingered Robot Hand using Elastic Elements as Joints

Yoichi OGAHARA[1], Yusuke KAWATO[2], Kenjiro TAKEMURA[3], Takashi MAENO[4]

[1]*Keio University, Yokohama, Japan, ogahara@mmm-keio.net*
[2]*Keio University, ykawato@mmm-keio.net*
[3]*Tokyo Institute of Technology, Yokohama, Japan, kenjiro@mmm-keio.net*
[4]*Keio University, maeno@mech.keio.ac.jp*

Key words: Elastic hinges, Miniature robot hand, Multi-finger, Feedforward control, Joint angle control

Abstract

This paper describes a new driving mechanism for a miniature robot hand. In developing miniature robot hands for dexterous manipulation, it is necessary to consider miniaturizing and minimalizing. The proposed mechanism uses elastic torsion springs and hinges as joints, and the finger is wire-driven from actuators placed outside the robot hand. First, the driving mechanism of a one joint finger is described, and the mechanism is applied to a five-fingered miniature robot hand. The robot hand is one-half the size of the hand of an adult male's, and has a total of eighteen degrees of freedom(DOF). The properties of the robot hand are discussed, and are shown to be an effective mechanism for miniature robot hands.

1. Introduction

20mmProjectionPulleyThumbfingerIndexfingerLittle
As the fabrication techniques of miniature parts such as micro-electrical mechanical systems (MEMS) are advancing at a very rapid rate, there is an increasing demand for a small-scaled manipulator to assemble such miniature parts. There have been many micromanipulators such as grippers which make simple grasping possible. However, a multi-DOF miniature robot hand is necessary in order to manipulate such objects with dexterity[1].

To accomplish complex tasks, the robot hand must have sufficient degrees of freedom. The robot hands that have been proposed previously exhibit a wide range of design solutions to this requirement. However, there are many problems when a similar mechanism is miniaturized. These former mechanisms can be divided into two categories, based on the location of the actuators.

When the actuators are placed inside the robot hand, this allows the robot hand to be used as a module, and the robot hand can be placed in any arbitrary place for use. However, there is a severe restriction on the size which makes miniaturization difficult, and it is difficult to drive every joint independently, as seen in DLR Hand II[2] and the Robonaut Hand[3]. When a similar mechanism is applied for small-scaled robot hands, there will be a limit to the size of the actuators and the sensors, and the output force will significantly decrease.

When the actuators are placed outside the robot hand, the robot hand becomes less bulky, with more design solutions. The driving force is generally transmitted by wires and pulleys, and the wires and pulleys are usually

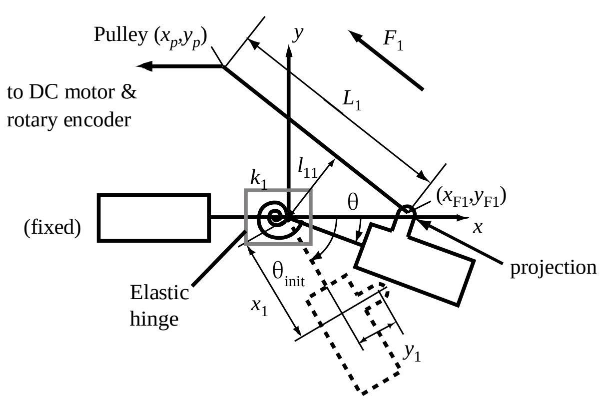

Figure 1: *Driving mechanism (One joint model)*

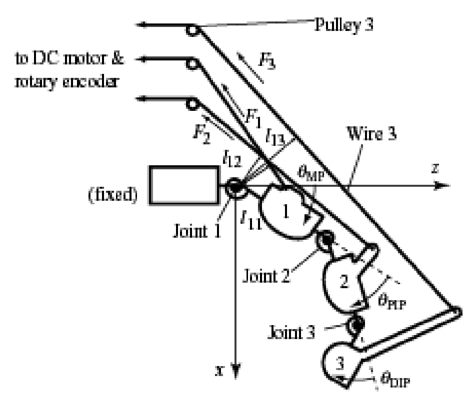

Figure 2: *Driving mechanism of a finger (Three joint model)*

Table 1: *Specifications of the developed miniature robot hand*

Finger	DOF	MP lateral [deg]	MP bending [deg]	PIP(IP) bending [deg]	DIP bending [deg]
Thumb	3	-12～60	-20～70	0～90	—
Index, Long, Ring	4	-30～30	-20～55	0～80	0～40
Little	3	-30～30	-20～55	0～80	—

placed inside the robot hand. However, the friction force caused by the pulleys increase, which greatly worsens the response of the robot hand.

For these reasons, the previously proposed mechanisms are too complex and bulky to be applied to miniature models. Therefore, a novel mechanism must be proposed to be used in small scaled robot hands. In this paper, a novel driving mechanism which uses elastic elements as joints is proposed. The kinematics and the characteristics of the mechanism are discussed. The mechanism is applied to a half scaled miniature robot hand, which is designed based on measurements of human hand movement. Then we carry out the joint angle control of the index finger. In the experiment, each joint is independently driven adopting feedforward control. Feedforward compensator in the control method is composed of an equation deduced by kinematics of the finger. Finally, the conclusions and future works are briefly discussed.

2. Driving Mechanism and Kinematics

The one joint model of the driving mechanism is shown in Fig. 1. Link 0 is fixed, and Link1 is connected by an elastic hinge. The joint is bent at its initial position of θ_{init}. A wire is connected to a projection of Link 1, and the wire is connected to a DC motor and rotary encoder, which is placed outside the robot hand. A pulley, assumed as a point, is placed outside the finger to minimize the number of pulleys and to reduce the friction force. The DC motor acts as an extensor, which stretches the joint, and the elastic element acts as a flexor. Therefore, the robot hand grasps an object using the elastic elements' restoring torque. This one joint model is applied to the robot hand for lateral movements of each finger.

The deflection angle of the joint can be calculated by either measuring the wire length or the wire tension. Therefore, by measuring both wire length and wire tension, the force when the finger touches an object can be detected.

The joint angle θ is calculated from the length of the wire L_1 by using the following equation. The symbols are defined in Fig. 1.

$$L_1 = \{x_1^2 + y_1^2 + x_p^2 + y_p^2 - 2x_p(x_1C_1 + y_1S_1) - 2y_p(-x_1S_1 + y_1C_1)\}^{1/2} \quad (1)$$

The joint angle can also be calculated from the wire tension F_j by using the following equation.

$$F_1 l_{11} = k_1(\theta_{\text{init}} - \theta_1) \quad (2)$$

l_{11} is the distance between joint 1 and wire 1, and can be solved by the following equation.

$$l_{11} = \frac{\partial L_1}{\partial \theta_1} \quad (3)$$

This mechanism is applied to the three joint model shown in Fig. 2. The moment around joint i caused by the DC motor is given by

$$\tau_{fi} = \sum_{j=i}^{3} F_j l_{ij} \quad (4)$$

where, F_j is the tension of wire i and l_{ij} is the distance between joint i and wire j. l_{ij} is solved by equation (5).

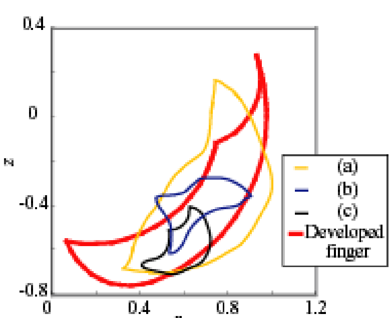

Figure 3: *Range of motion (Thumb)*

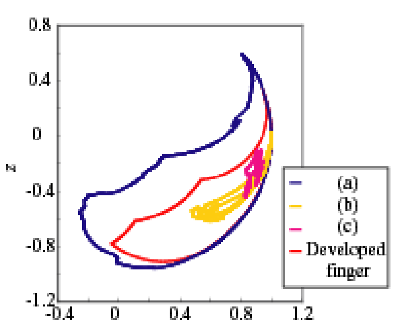

Figure 4: *Range of motion (Index finger)*

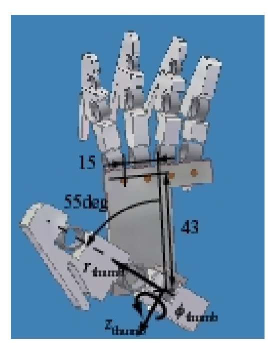

Figure 5: *Five fingered model of developed robot hand*

$$l_{ij} = \frac{\partial L_j}{\partial \theta_i} \tag{5}$$

The restoring torque τ_{ki} of the elastic element at joint i is given by

$$\tau_{ki} = k_i (\theta_{\text{init}} - \theta_i) \tag{6}$$

where, θ_i is the joint angle and k_i is the spring coefficient of the elastic element. The joint angle can be calculated by solving the following static balance equation for each joint.

$$\tau_{fi} = \tau_{ki} \tag{7}$$

By changing the initial position of the elastic elements, the size of the projection, and the position of the pulley, it is possible to optimize the specifications for each finger.

The following characteristics are expected by applying this mechanism to miniature robot hands[4]:

(a) Compliant mechanism allowing greater shock tolerance, allowing less damage during inadvertent contact
(b) Makes stable force control more easy to achieve
(c) Simplifies structure design, making it easy to be manufactured
(d) Reduces friction by using minimum number of pulleys
(e) Due to scaling, the robot hand can handle objects that are relatively more massive

When the human performs dexterous manipulation, the finger compliance is raised to an extremely high level to adapt the hand to the object and follow external forces[5]. This mechanism is adequate for precision grasps, for it allows high finger compliance mechanically.

3. Design and Manufacturing

The anthropomorphic robot hand is approximately one-half the size of an adult male's, and is designed to manipulate objects of sizes between 10 mm to 45 mm. Each finger is designed to have a maximum output force of at least 1.0 N at the fingertip, and the output force of the thumb to be considerably larger. The elastic element of each joint is composed of elastic torsion springs and hinges made of polycaprolactone (PCL).

The robot hand is designed based on measurements of the human hand motion. The measurements were performed for the following three conditions:

(a) Non-constraint motion
(b) Motion for handling a ϕ20 mm sphere
(c) Motion for handling a ϕ90 mm sphere

These measurements were performed for the thumb and the index finger, and the results are shown in Fig. 3 and Fig. 4 respectively. The measured results are transferred to dimensionless parameters, where 1 is the length of each finger. In Fig. 3, the data is transferred to polar coordinates, as defined in Fig. 5. In Fig. 4, the origin of the coordinates is at the MP joint of the index finger.

Based on these measured results, the maximum range of motion for each joint was decided. The specifications are shown in Table 1. From Fig. 3 and Fig. 4, it is clear that the developed three DOF thumb's and four DOF index finger's range of motion satisfies that of the humans'. Therefore, we can conclude that the developed robot hand can simulate the finger motion of humans when manipulating objects.

The other three fingers are designed based on the measured results of the index finger. The thumb and little finger has three DOF, and the index, long, and ring fingers have four DOF.

The sizes of the projections and the placement of the pulleys were decided so that they do not come in contact. The specifications of the springs were decided to meet the requirements.

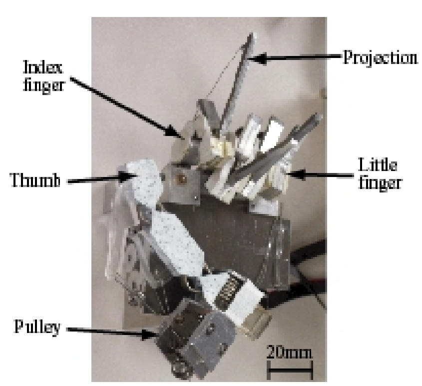

Figure 6: *Developed robot hand*

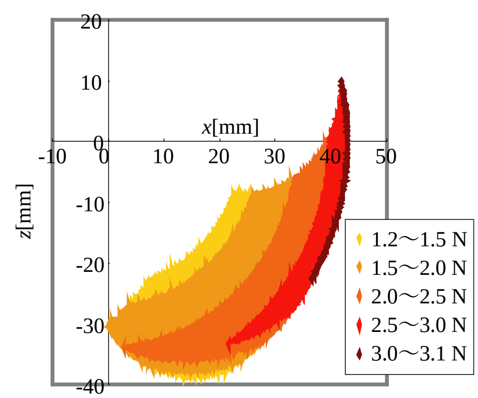

Figure 7: *Maximum output force at fingertip (Index finger)*

4. Evaluation of Robot Hand

The developed miniature robot hand is shown in Fig. 6. The robot hand has a total of 18 degrees of freedom, and is connected to 18 actuators and 18 rotary encoders. The robot hand is 250 g excluding the actuators and rotary encoders.

The maximum output force of the index finger is shown in Fig. 7. The figure shows the calculated result of the force at the fingertip when $\theta_2 = 2 \times \theta_3$. The maximum output force is between 1.2 N and 3.1 N, and becomes larger as the finger is in a more extended state. The maximum force for the thumb is 5.0 N, which is larger than the other fingers.

The precision of the position control was tested for the index finger. The test was performed by controlling the length of each wire, which was measured by using potentiometers. The average position control error was 0.41 mm at the fingertip, with standard deviation of 0.20 mm. The main causes of the error are the low resolving power of the potentiometer and the stretching of the wires. For the robot hand, rotary encoders with higher resolution will be used to improve its position accuracy.

5. Control Method

This section introduces control method for the finger joints of the robot hand. Since the index finger has a standard structure, we choose it as a controlled object, while the control method we propose can be applied to other fingers. As shown in Fig. 2, motions of joint 1, 2 and 3 are coupled where three degree-of-freedom generates flextion movement and extension movement. On the other hand, one degree-of-freedom in lateroflexion movement is not coupled with motions of joint 1, 2 and 3. Therefore we aim to control angles of joint 1, 2 and 3 of the index finger, neglect one degree-of-freedom in lateroflexion movement. Variables of the index finger are defined in vector form as

$$\boldsymbol{\theta} = \left(\theta_1 \quad \theta_2 \quad \theta_3\right)^T$$
$$\boldsymbol{\theta}_m = \left(\theta_{m1} \quad \theta_{m2} \quad \theta_{m3}\right)^T$$
$$\mathbf{F} = \left(F_1 \quad F_2 \quad F_3\right)^T$$
$$\boldsymbol{\tau}_f = \left(\tau_{f1} \quad \tau_{f2} \quad \tau_{f3}\right)^T$$
$$\boldsymbol{\tau}_k = \left(\tau_{k1} \quad \tau_{k2} \quad \tau_{k3}\right)^T$$

where, $\boldsymbol{\theta}$ is a joint angle vector of the finger, $\boldsymbol{\theta}_m$ is a rotational angle vector of motors, $\mathbf{F}$ is a wire tension vector, $\boldsymbol{\tau}_f$ is a joint torque vector around the finger joint caused by a wire tension, and $\boldsymbol{\tau}_k$ is a restoring torque vector of an elastic element. Clockwise rotation is defined to be positive direction of a torque.

For position control of the finger joint we propose feedforward control, a block diagram of the feedforward control is shown in Fig. 8 where **A**(s) denotes a transfer function which converts the joint angle vector of the finger into the rotational angle vector of motors. $\mathbf{G}_c$(s) is a PID compensator. **R**(s) is a feedforward compensator. **T**(s) is a transfer function which converts the wire tension vector into the joint torque vector. **G**(s) is a transfer function of the finger. **A**(s) is deduced from a geometric relation between joint angles and pulleys as described in section 2. $\mathbf{G}_c$ (s) is expressed as

$$\mathbf{G}_c(s) = \mathbf{K}_p + \mathbf{K}_d s + \frac{\mathbf{K}_i}{s} \qquad (8)$$

where, $\mathbf{K}_p, \mathbf{K}_d$ and $\mathbf{K}_i$ are diagonal matrices.

Now we consider a static balance of the finger to deduce **T**(s) and **R**(s). We express a static balance of the finger as follows:

$$\boldsymbol{\tau}_k = \boldsymbol{\tau}_f\left(\boldsymbol{\theta}\right) \qquad (9)$$

Here $\boldsymbol{\tau}_f(\boldsymbol{\theta})$ is deduced from the principle of virtual work as follows:

$$\tau_{f1} d\theta_1 + \tau_{f2} d\theta_2 + \tau_{f3} d\theta_3 = F_1 dL_1 + F_2 dL_2 + F_3 dL_3 \qquad (10)$$

Also the matrix representation is described as

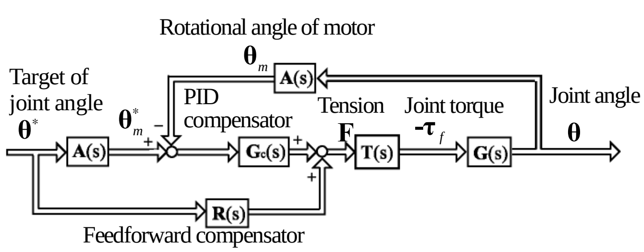

Figure 8: *Block diagram of feedforward control*

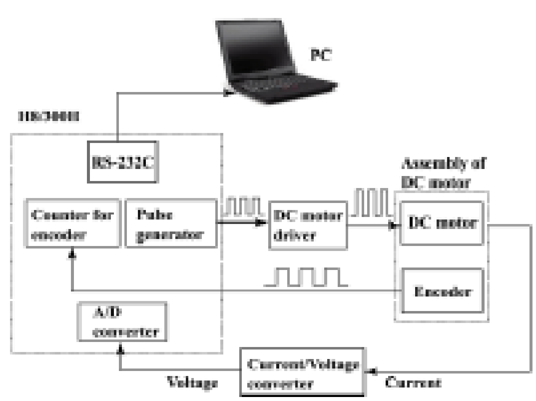

Figure 9: *Control system of the experiment*

$$\boldsymbol{\tau}_f(\boldsymbol{\theta}) = \mathbf{H}(\boldsymbol{\theta})\mathbf{F} \tag{11}$$

where, $\mathbf{H}(\boldsymbol{\theta}) \in R^{3\times3}$ is a function matrix of the joint angle vector. In short, the wire tension vector is converted into torque vector around the finger joint caused by the wire tension using equation (11). Hence, **T**(s) is deduced by performing the Laplace transform of equation (11).

Next the following equation is deduced from equations (9) and (11).

$$\mathbf{F} = \mathbf{H}(\boldsymbol{\theta})^{-1}\boldsymbol{\tau}_k \tag{12}$$

In this study we use linear torsion springs and hinges as elastic elements. A hinge has nonlinear characteristic between the restoring torque and the joint angle. Here we approximate elastic element of the finger joint to have linear characteristic. Because the hinge is less effective than the linear torsion spring as elastic element, we neglect the effect of the hinge. Hence, we obtain

$$\boldsymbol{\tau}_k(\boldsymbol{\theta}) = \begin{pmatrix} k_1(\theta_{init1} - \theta_1) \\ k_2(\theta_{init2} - \theta_2) \\ k_3(\theta_{init3} - \theta_3) \end{pmatrix} = \mathbf{K}\Delta\boldsymbol{\theta} \tag{13}$$

where,

$$\mathbf{K} = \begin{pmatrix} k_1 & 0 & 0 \\ 0 & k_2 & 0 \\ 0 & 0 & k_3 \end{pmatrix}$$

$$\Delta\boldsymbol{\theta} = \begin{pmatrix} \theta_{init1} - \theta_1 \\ \theta_{init2} - \theta_2 \\ \theta_{init3} - \theta_3 \end{pmatrix}$$

Then equation (12) can be rewritten as follows:

$$\mathbf{F} = \mathbf{H}(\boldsymbol{\theta})^{-1}\mathbf{K}\Delta\boldsymbol{\theta} \tag{14}$$

R(s) is deduced by performing the Laplace transform of equation (14).

Finally we deduce **G**(s) using Lagrangian. We model the finger joint as a spring-damper model. The Lagrange's equation of motion is shown as

$$\mathbf{I}(\boldsymbol{\theta})\ddot{\boldsymbol{\theta}} + \mathbf{C}\dot{\boldsymbol{\theta}} - \mathbf{K}\Delta\boldsymbol{\theta} + \mathbf{q}(\dot{\boldsymbol{\theta}}, \boldsymbol{\theta}) = \boldsymbol{\tau}_f(\boldsymbol{\theta}) \tag{15}$$

where, $\mathbf{I}(\boldsymbol{\theta}) \in R^{3\times3}$ is a inertia matrix, $\mathbf{C} \in R^{3\times3}$ is a diagonal damping matrix, $\mathbf{q}(\dot{\boldsymbol{\theta}}, \boldsymbol{\theta}) \in R^{3\times3}$ is a nonlinear term including torques caused by friction and gravity, and $\boldsymbol{\tau}_f(\boldsymbol{\theta})$ is a driving torque. Then **G**(s) is deduced by performing the Laplace transform of equation (15).

We apply feedforward control method with the equations deduced in this section to control joint angles in the experiment we describe in the next section.

6. Experiment

6.1 Experimental setup

We carried the angle control experiment of the finger using feedforward control. The configuration of the system for the control experiment is shown in Fig. 9. The microcomputer H8/300H (HITACHI Inc.) is used as a controller. Coreless DC motors (Maxon Inc.) are used as motors. Rotary encoders (Maxon Inc.) and a counter of microcomputer are used to measure the rotation angle of the motor. To drive the motors PWM control was used with TA8440H (TOSHIBA Inc.) as a motor driver. The torque from the DC motor is calculated by multiplying the measured current which flow in the DC motor by the torque constant of the DC motor. A/D converter and Current/Voltage converter are used to measure the current. Obtained information such as joint angles and torques of DC motors is displayed on the PC using RS-232C.

PWM control is executed every 300 μs. A desired duty ratio is calculated by the torque control using PI controller. Then feedforward control is executed every 2ms. A desired torque is calculated using feedforward compensator and PID compensator, where, each gain of PI controller and PID compensator is decided by trial and error.

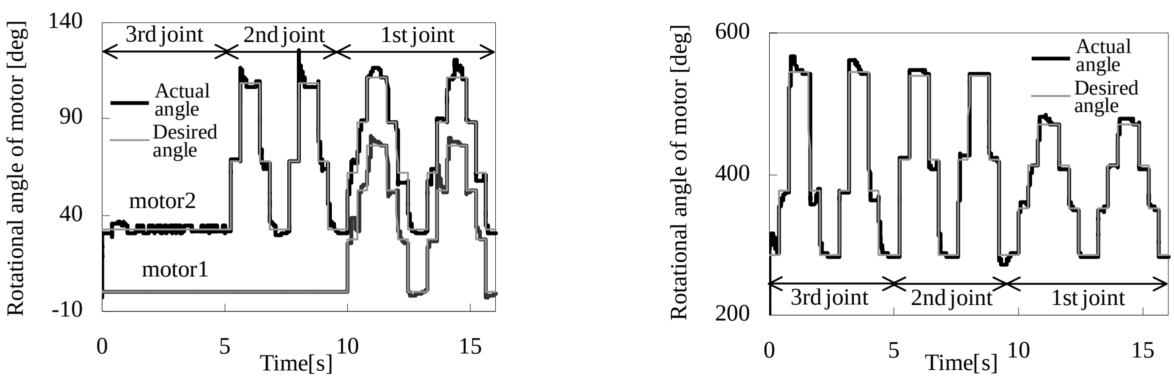

(a) motor1,2 *(b) motor3*

Figure 10: *Rotational angle trajectories of motor during feedforward control*

6.2 Results

In this experiment, each joint of the finger was independently driven. The desired value of joint angle changes step-like as shown as gray line in Fig. 10. The results of tracking control to desired value is also shown as bold line in Fig. 10. Fig. 10 (a) shows the rotational angles of motor 1 and motor 2 under feedforward tracking control. Fig. 10 (b) shows the rotational angle of motor 3. Each Gain for PID compensator are as follows:

$$\mathbf{K}_p = \begin{pmatrix} 482 & 0 & 0 \\ 0 & 410 & 0 \\ 0 & 0 & 217 \end{pmatrix} [\text{mN/deg}]$$

$$\mathbf{K}_d = \begin{pmatrix} 2.89 & 0 & 0 \\ 0 & 3.13 & 0 \\ 0 & 0 & 2.41 \end{pmatrix} [\text{mN}\cdot\text{s/deg}]$$

$$\mathbf{K}_i = \begin{pmatrix} 28.9 & 0 & 0 \\ 0 & 14.5 & 0 \\ 0 & 0 & 4.82 \end{pmatrix} [\text{mN/s}\cdot\text{deg}]$$

As shown in Fig. 10, actual angles appear to follow desired angles. It is demonstrated that the feedforward control method is effective within the range measured in this study. However angle errors in steady state are not negligible. It seems to be attributed to the friction forces between the pulley and the motor. There are modeling errors on elastic elements of the finger joint as well. To settle these problems, we should reduce friction force or should consider the nonlinearity for joint angle of elastic element. A control method using neural network as feedforward compensator is effective for joint angle control.

7. Conclusions and Future Works

A novel mechanism for miniature robot hands is proposed, and is shown to have suitable characteristics for dexterous manipulation. A half-scaled miniature robot hand is designed and developed, and are shown to satisfy the design conditions. Feedforward control method is adopted to control joint angles of the index finger in the experiment. It is demonstrated that the control is effective within this study.

Further experiment will be conducted to test its usefulness in practical applications. We are planning to use this robot hand for master-slave systems to manipulate small objects. A smaller robot hand will be developed to verify the validity of the mechanism and control method.

Acknowledgement

This study was supported in-part by a Grant-in-Aid from Frontier Research from Keio Leading-edge Laboratory of Science and Technology.

References

[1] Antonio Bicchi: Hands for Dexterous Manipulation and Robust Grasping: A Difficult Road Toward Simplicity, IEEE Transactions on Robotics and Automation, Vol.16, No.6, pp.652-662, (2000)

[2] J. Butterfass, M. Grebenstein, H. Lieu, G. Hirzinger: DLR-Hand II: Next Generation of a Dexterous Robot Hand, Proceedings of the 2001 IEEE International Conference on Robotics and Automation, pp.109-114, (2001)

[3] C.S. Lovchik, M.A. Diftler：The Robonaut Hand: A Dexterous Robot Hand For Space, Proceedings of the 1999 IEEE International Conference on Robotics and Automation, pp.907-912,(1999)

[4] Gill A. Pratt et al: Stiffness Isn’t Everything, ISER’95, pp.253-262, (1995)

[5] Shigeki Sugano, Hideyo Namimoto, Ichiro Kato: Compliance Control Using Finger-Arm Coordination Analysis of Human Motion in Constraint Work, Int. Conf. Advanced Robotics, pp.456-462, (1991)